KSCE Journal of Civil Engineering (2022) 26(11):4737-4745
DOI 10.1007/s12205-022-0318-8

pISSN 1226-7988, eISSN 1976-3808
www.springer.com/12205

Structural Engineering

Condition Assessment of Railway Bridge Sliding Bearing Using Alternating Vehicle Longitudinal Excitation

Naijie Han[a], **Hao Zhang**[b], **Weigang Zhao**[b], **and Liming Zhou**[b]

[a]*School of Civil Engineering, Shijiazhuang Tiedao University, Shijiazhuang 050043, China*
[b]*School of Safety Engineering and Emergency Management, Shijiazhuang Tiedao University, Shijiazhuang 050043, China*

ARTICLE HISTORY

Received 2 March 2022
Revised 30 May 2022
Accepted 14 June 2022
Published Online 7 September 2022

KEYWORDS

Structural health monitoring
Railway bridge
Bearing friction
Bearing working performance
Vehicle longitudinal effect

ABSTRACT

The identification of maximum bearing friction is critical to working performance assessment of bridge sliding bearings. The friction-displacement hysteresis model was used for the bearing working performance (BWP) assessment. In this study, the bearing longitudinal displacement (BLD) hysteresis model is established for the sliding bearing system, introducing bearing friction and vehicle longitudinal effect. A novel approach for BWP assessment is presented using alternating vehicle longitudinal excitation. First, bearing friction and vehicle longitudinal effect were introduced to establish the hysteresis model of BLD. Subsequently, the evaluation index and the assessment approach were proposed for BWP assessment using the alternating vehicle longitudinal excitation. Finally, the assessment approach for BWP was applied to a real-world railway bridge. The results show that temperature-displacement relationship model for BWP assessment is unapplicable under significant vehicle longitudinal effects. On the contrary, the BLD induced by alternating vehicle longitudinal excitation can identify the degradation of the BWP when vehicle longitudinal excitation overcomes maximum bearing friction.

1. Introduction

Well bearing working performance (BWP) contributes to improving the longitudinal deformation capacity of bridge, which facilitates bridges to accommodate external adverse impact (e.g., earthquake, vehicle loads, extreme temperature). Owing to the repetitive impacts of vehicle loads and periodic variation of temperature, the degradation of BWP has been increasingly observed (Lima and Brito, 2009; Brownjohn et al., 2015; Yarnold et al., 2015; Guo et al., 2016; Sun and Zhang, 2016). The degradation of BWP (e.g., the increase of maximum bearing friction) weakens the longitudinal deformation capacity of bridge. Therefore, keeping track of BWP is an urgent requirement for bridge maintenance.

Bridge condition can be evaluated by the structural health monitoring system during bridge operation (Ni et al., 2007; Li et al., 2022; Liang et al., 2022). The temperature-displacement relationship model (TDRM) was used for detecting the degradation of BWP (Murphy and Yarnold, 2018; Han et al., 2021a), whose feasibility has been demonstrated in various types of bridges, such as arch bridges (Yarnold et al., 2015), cable stayed bridges (Huang et al., 2018; Ni et al., 2020; Chen et al., 2021), continuous bridges (Wang et al., 2015; Murphy and Yarnold, 2018; Alexander and Yarnold, 2020; Garcia-Sanchez et al., 2020; Wu et al., 2021; Han et al., 2021b) and suspension bridge (Xia et al., 2020). Data-driven techniques, such as multiple linear regression (Wang et al., 2015), canonical correlation analysis (Huang et al., 2018), support vector machine (Chen et al., 2021), principal component analysis (Garcia-Sanchez et al., 2020), Bayesian estimation (Ni et al., 2020), were applied to anomaly detection of BWP. In summary, TDRM is a widely accepted tool for BWP assessment using field monitoring data. Among those researches, the effect of bearing friction on bearing longitudinal displacement (BLD) has received increasing interest (Yarnold and Moon, 2015; Yarnold et al., 2015; Garcia-Sanchez et al., 2020; Han et al., 2021b), showing that maximum bearing friction is a critical parameter of BWP, which can be recognized by TDRM.

There is a nonlinear hysteresis relationship between BLD and bearing friction (Filipov et al., 2013; Yue et al., 2017; Jia et al.,

CORRESPONDENCE Weigang Zhao ✉ zhaowg@stdu.edu.cn 🏢 School of Safety Engineering and Emergency Management, Shijiazhuang Tiedao University, Shijiazhuang 050043, China

2018; Quaglini et al., 2018; Wen et al., 2019). Obviously, The maximum bearing friction can be identified by TDRM when BLD is induced by temperature only. However, the moving trains can induce longitudinal internal forces in the girder also, which can induce BLD in a way. Srinivas (Srinivas et al., 2013) carried out an experimental investigation, which indicated that the tractive effort of trains can change the longitudinal internal forces of girder. Liu et al. (2019) established a track–bridge–pier–foundation model, adopting the nonlinear spring element to simulate the sliding bearings. The research showed that the trains longitudinal effect caused the variation of bearing friction and BLD. Han (Han et al., 2021b) confirmed that moving trains can induce BLD variation through monitoring data of a railway bridge.

Because of the nonlinear hysteresis relationship between BLD and bearing friction, both vehicle-induced BLD and temperature-induce BLD have effect on bearing friction. Consequently, BWP assessment using TDRM is controversial when the BLD is significantly affected by trains longitudinal effects. Nonetheless, some researches (Wang et al., 2015; Wu et al., 2021) treated vehicle-induced BLD as invalid information. In this study, a hysteresis model of BLD under vehicle longitudinal effect was presented in this paper, and a novel approach for a railway bridge BWP assessment is proposed using alternating vehicle longitudinal excitation. The rest of the paper is organized as follows. First, a hysteresis model of BLD was presented by introducing bearing friction and vehicle longitudinal effect. Secondly, the approach for BWP assessment and corresponding evaluation index were proposed based on the hysteresis model. Thirdly, the hysteresis model was verified by field monitoring data. The approach was applied to a real-world bridge. Finally, some suggestions on BWP assessment were presented for further research.

2. BLD Response under Vehicle Longitudinal Force

The nomenclature for Figs. 1, 2, Eq. (1) was shown in Table 1.

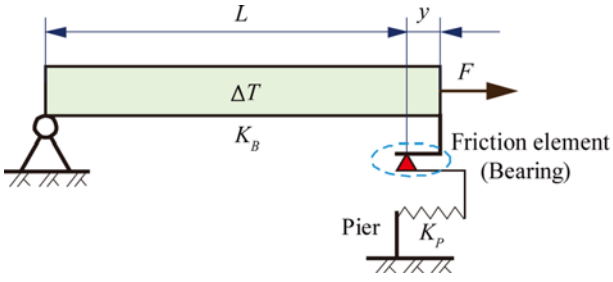

Fig. 1. Caculation Illstration for BLD

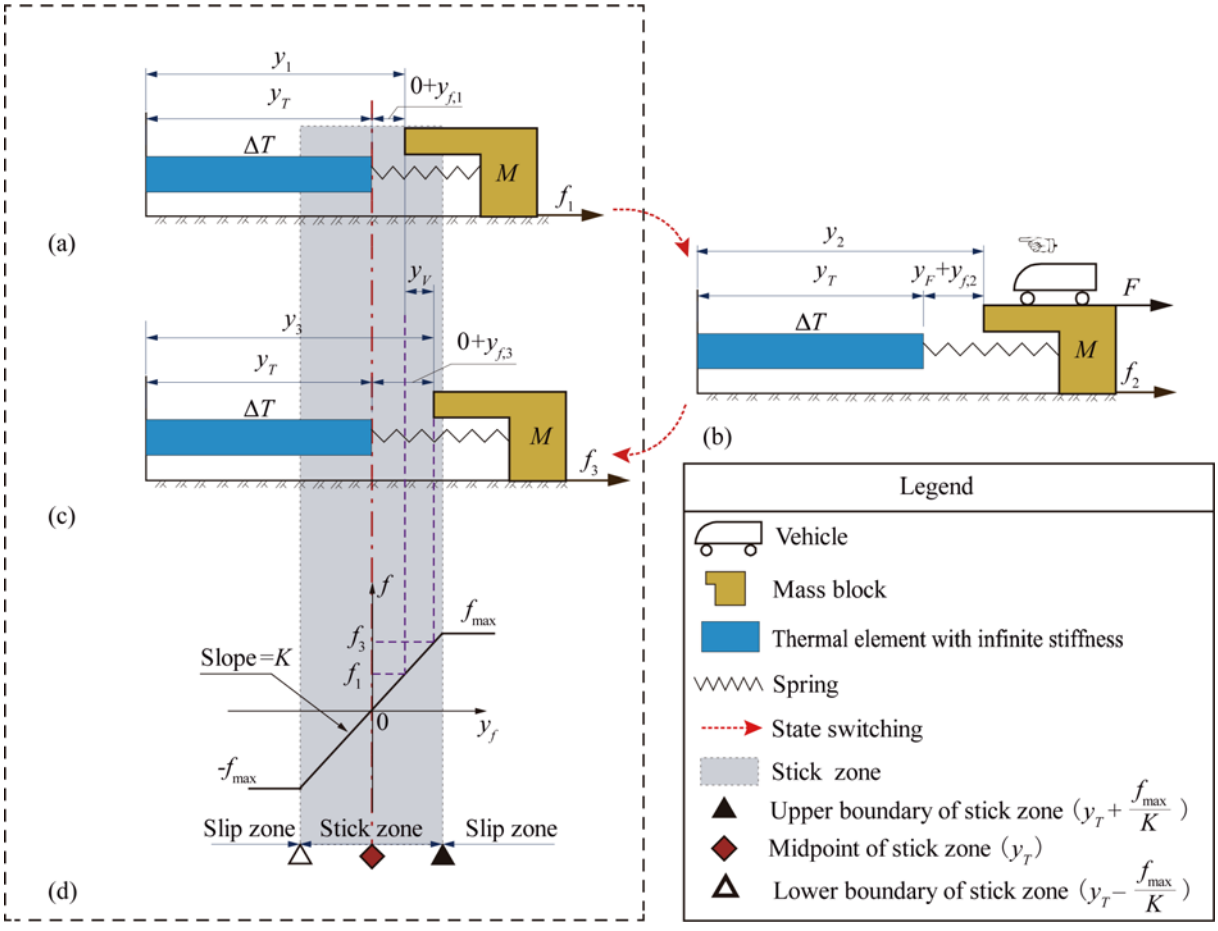

Fig. 2. BLD Computational Model Introducing Temperature, Friction and VLF: (a) Initial State, (b) VLF Loading State, (c) VLF Unloading State, (d) Slip Zone and Stick Zone Without VLF

Table 1. Nomenclature for Figs. 1, 2 and Eq. (1)

No.	Name	Physical meanings
1	ΔT	= Temperature variation of the beam
2	L	= The original length of the beam
3	y	= BLD
4	F	= Vehicle longitudinal force (VLF)
5	f	= The bearing friction
6	M	= The mass of the beam assigned to the bearing
7	K_B	= Longitudinal stiffness of beam
8	K_P	= Longitudinal stiffness of pier top
9	K	= Series stiffness of beam and pier, i.e., $K_B K_P /(K_B + K_P)$
10	f_1	= The bearing friction in initial state
11	f_2	= The bearing friction in VLF loading state
12	f_3	= The bearing friction in VLF unloading state
13	f_{max}	= The maximum bearing friction, i.e. dynamic friction.
14	y_1	= BLD in initial state
15	y_2	= BLD in VLF loading state
16	y_3	= BLD in VLF unloading state
17	y_T	= Temperature-induced BLD
18	y_F	= VLF-induced BLD
19	y_f	= Restrained BLD by friction
20	y_{fi} (i=1,2,3)	= Restrained BLD by f_i (i=1,2,3)
21	y_V	= The BLD variation after vehicle passes through the bridge

The longitudinal load on the beam induced by moving vehicle is defined as vehicle longitudinal force (VLF). The BLD (y) is affected by ΔT, f, and F, shown in Fig. 1. Consequently, BLD (y) is made up of temperature-induced BLD (y_T), friction-induced BLD (y_f) and VLF-induced BLD (y_F) under quasi-static process.

The variation of BLD was decomposed into three stages: initial state (Fig. 2(a)), VLF loading state (Fig. 2(b)), and VLF unloading state (Fig. 2(c)). The relationship between variates can be expressed as Eq. (1).

$$\begin{cases} y_i - y_T = y_F + y_{f,i} \\ y_T = \alpha \Delta T L \\ y_{f,i} = f_i / K \qquad (i = 1,2,3) \\ y_F \propto F / K_B \\ f_{\max} = \mu M g \end{cases} \tag{1}$$

where α is the expansion coefficient; μ is the friction coefficient.

The bearing friction displayed a nonlinear stick-slip displacement mechanism without VLF: stick zone (static friction) and slip zone (dynamic friction) (Fig. 2(d)) (Yarnold and Moon, 2015; Yarnold et al., 2015; Alexander and Yarnold, 2020; Han et al., 2021b). VLF is loaded on the beam longitudinally when vehicles pass through bridge (Fig. 2(b)). After VLF is removed as a shortlived load (Fig. 2(c)), the temperature hardly changes at all, and the bearing stays in the stick zone (i.e., static friction). Thus, the BLD variation y_V (Figs. 2(a), 2(c)) is expressed as

$$y_V = y_3 - y_1 = \frac{f_3 - f_1}{K} \tag{2}$$

According to Eq. (2), y_V is the result of bearing friction variation after vehicle pass through bridge. Therefore, when the BLD variation occurs after vehicle passes the bridge, the vehicle effect must be considered for identifying f_{max}. In this case, the formula for BLD was established introducing y_F and f_{max}, expressed as Eq. (3).

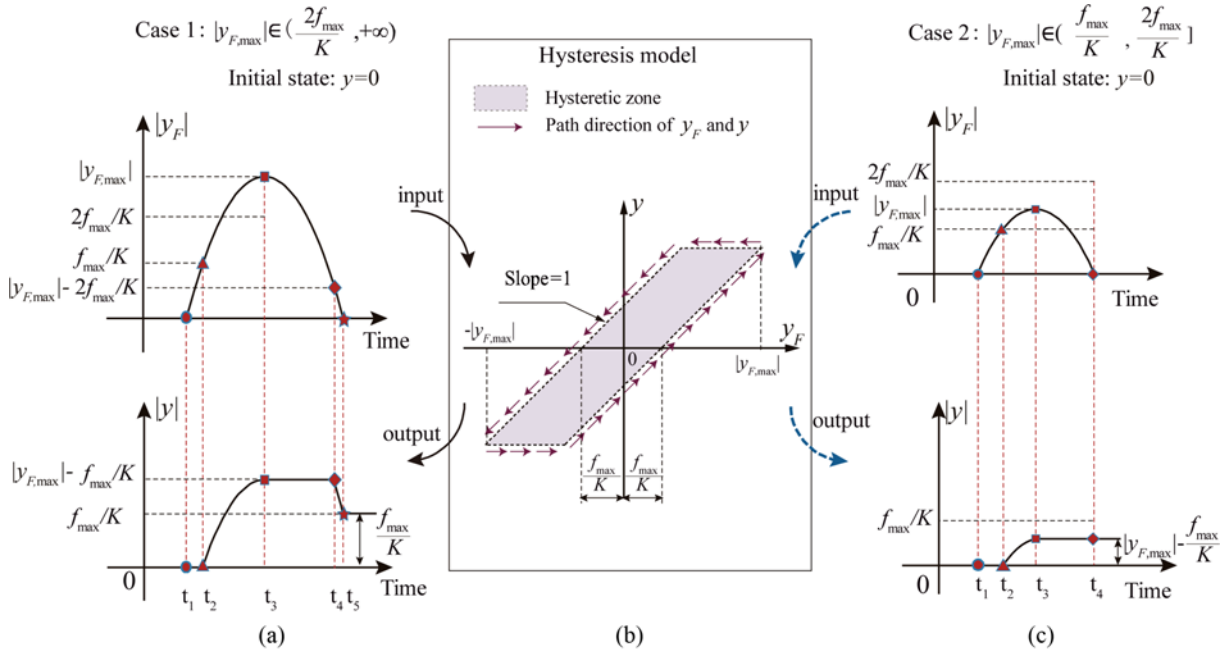

Fig. 3. The Hysteresis Model: (a) Case1 Input–Output, (b) Hysteresis Model, (c) Case2 Input–Output

$$\begin{cases} y = y_F - \dfrac{f_{\max}}{K} \cdot \operatorname{sign}(y_F - y), & |y - y_F| \geq \dfrac{f_{\max}}{K} \\ \dfrac{\mathrm{d}\, y}{\mathrm{d}\, y_F} = 0, & |y - y_F| < \dfrac{f_{\max}}{K} \end{cases} \tag{3}$$

Further, the Eq. (3) can be represented by a hysteresis model shown in Fig. 3(b). For instance, setting the initial value of y is zero, two cases of input–out signal were shown in Figs. 3(a) and 3(c), where $y_{F,\max}$ is the maximum strength of input signal (y_F). When the $|y_{F,\max}|$ is less than $f_{\max}/K$, the output signal (y) is zero always, which was not necessary to be shown.

3. Evaluation Index Based on Alternating Vehicle Longitudinal Excitation

3.1 The Relationship between y_V and $f_{\max}$

In this section, an evaluation index was proposed for identifying $f_{\max}$ using alternating vehicle longitudinal excitation. First, we discussed the BLD (y) according to two cases, shown in Fig. 4.

Case 1: $|y_{F,\max}| \in (2f_{\max}/K, +\infty)$.

The maximum BLD is greater than $f_{\max}/K$ (Figs. 4(a), 4(c)) when VLF loads. After the VLF unloads, only $f_{\max}$ acts on the girder, and the spring internal force must be released to balance $f_{\max}$. Consequently, the bearing slides to the closest boundary of the stick zone (Figs. 4(b), 4(d)), so y can be calculated as follows

$$y = \frac{f_{\max}}{K} \operatorname{sign}(F) \tag{4}$$

Case 2: $|y_{F,\max}| \in (f_{\max}/K, 2f_{\max}/K]$. The maximum BLD is less than $f_{\max}/K$ when VLF loads (Figs. 4(a), 4(c)). BLD remains static after the VLF unloads (Figs. 4(b), 4(d)); y can be calculated as follows

$$y = \left(|y_{F,\max}| - \frac{f_{\max}}{K} \right) \operatorname{sign}(F) \tag{5}$$

According to Eqs. (4) and (5), after VLF unloads, y can be determined by the $y_{F,\max}$ and $f_{\max}/K$ only. In addition, y_V is the difference between the initial value and the final value of y. Consequently, both previous vehicle effect and current vehicle effect should be analyzed. Assume that $|y_{F,\max}|$ is constant. Four vehicle driving cases and friction conversion were shown in Fig. 5. Four vehicle driving cases were defined as follow.

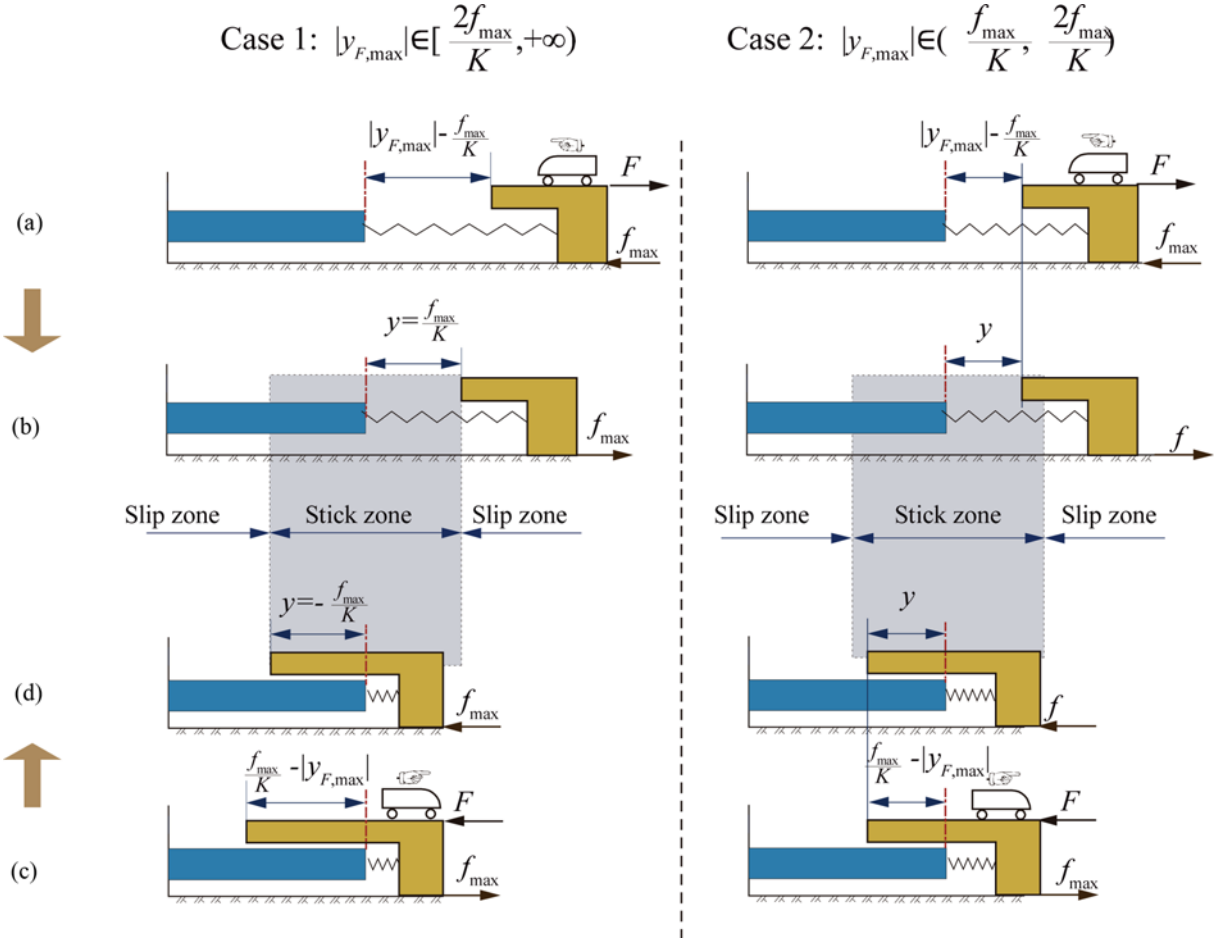

Fig. 4. BLD Response Under VLF: (a) The Positive VLF Loads, (b) The Positive VLF Unloads, (c) The Negative VLF Loads, (d) The Negative VLF Unloads

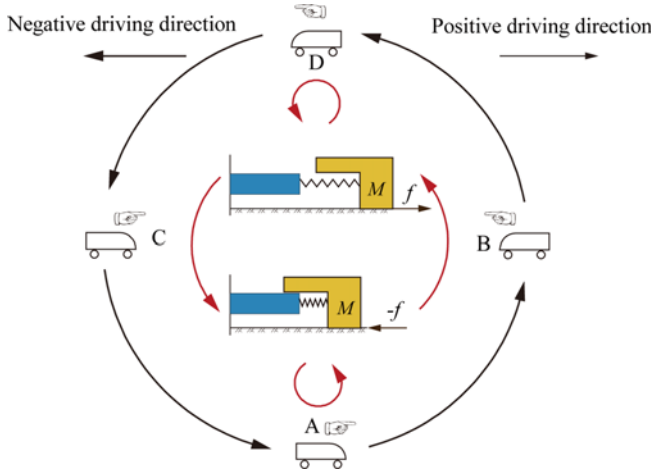

Fig. 5. Vehicle Driving Cases and Friction Conversion (the head of the black arrow line represents the current driving direction of the vehicle; the end of the black arrow line represents the previous driving direction of the vehicle; the red arrow represents the friction conversion)

Case A: both driving direction of previous vehicle and driving direction of current vehicle are positive.

Case B: driving direction of previous vehicle is positive, driving direction of current vehicle is negative.

Case C: driving direction of previous vehicle is negative, driving direction of current vehicle is positive.

Case D: both driving direction of previous vehicle and driving direction of current vehicle are negative.

Case A and case D are repetitive excitation, while case B and case C are alternating excitation. Based on the hysteresis model (Fig. 5), y_V is zero under case A and case D. In contrast, y_V arises under case B and case C, expressed by Eq. (6), where Y_V is the oscillation range of BLD under case B and case C. Thus, $f_{\max}$ can be determined from oscillation range (Y_V) induced by case B and case C. In this study, the excitation of two adjacent vehicles driving in opposite directions (case B and case C) is defined as "alternating VLF".

$$Y_V = |y_V| = \begin{cases} Y_{V,\max} = 2\dfrac{f_{\max}}{K}, & |y_{F,\max}| \in \left(\dfrac{2f_{\max}}{K}, +\infty\right) \\ 2\left(|y_{F,\max}| - \dfrac{f_{\max}}{K}\right), & |y_{F,\max}| \in \left[\dfrac{f_{\max}}{K}, \dfrac{2f_{\max}}{K}\right] \end{cases} \tag{6}$$

3.2 Probabilistic Evaluation Index

Considering $y_{F,\max}$ is a random variable, we defined Π as

$$\Pi = K y_{F,\max} \tag{7}$$

The probability of Π is defined as $P_\Pi(\Pi)$, and probability density of Π is defined as $p_\Pi(\Pi)$. Assume that $P_\Pi(\Pi)$ is independent of the direction of F. In view of the situation of alternating VLF, two variables are defined: Π_a is induced by the previous passing vehicle, and Π_b is induced by the current passing vehicle, Π_a and Π_b are in opposite directions. The event wherein both $|\Pi_a|$ and $|\Pi_b|$ are greater than $2f_{\max}$ is defined as Θ, and the probability of Θ is expressed as follows

$$\begin{aligned} P(\Theta) &= P_\Pi\left(|\Pi_a| \geq 2f_{\max}, |\Pi_b| \geq 2f_{\max}\right) \\ &= P_\Pi\left(|\Pi| \geq 2f_{\max}\right)^2 \\ &= \int_{2f_{\max}}^{+\infty} {p_\Pi}^2(|\Pi|)d\Pi \end{aligned} \tag{8}$$

$\overline{\Theta}$ is a complementary set of Θ, and there are three categories of $\overline{\Theta}$, as follows

(1) $\overline{\Theta}_1$: $|\Pi_a| \in (2f_{\max}, +\infty)$, $|\Pi_b| \in (f_{\max}, 2f_{\max}]$.
(2) $\overline{\Theta}_2$: $|\Pi_a| \in (f_{\max}, 2f_{\max}]$, $|\Pi_b| \in (2f_{\max}, +\infty)$.
(3) $\overline{\Theta}_3$: $|\Pi_a| \in (f_{\max}, 2f_{\max}]$, $|\Pi_b| \in (f_{\max}, 2f_{\max}]$.

The probability of $\overline{\Theta}_1$ and $\overline{\Theta}_2$ are as follows

$$P(\overline{\Theta}_1) = P_\Pi(\overline{\Theta}_2) = \int_{2f_{\max}}^{+\infty} p_\Pi(|\Pi|)d\Pi \cdot \int_{f_{\max}}^{2f_{\max}} p_\Pi(|\Pi|)d\Pi \tag{9}$$

The probability of $\overline{\Theta}_3$ is as follows

$$P(\overline{\Theta}_3) = \int_{f_{\max}}^{2f_{\max}} {p_\Pi}^2(|\Pi|)d\Pi \tag{10}$$

Based on the Bayesian formula, the probability density of Y_V is expressed as follows

$$\begin{aligned} p_Y(Y_V) = {} & p_Y(Y_V \mid \Theta)P(\Theta) \\ & + p_Y(Y_V \mid \overline{\Theta}_1)P(\overline{\Theta}_1) \\ & + p_Y(Y_V \mid \overline{\Theta}_2)P(\overline{\Theta}_2) \\ & + p_Y(Y_V \mid \overline{\Theta}_3)P(\overline{\Theta}_3) \end{aligned} \tag{11}$$

Define the event X as the $f_{\max}$ increasing by x ($x > 0$). The prior information is that the BWP degraded as long as bearing entry into service; thus, the probability of event X is expressed as Eq. (12) while bearings are on service.

$$P(\mathrm{X}) = 1 \tag{12}$$

$p_Y(Y_V, \mathrm{X})$ is the joint probability density of Y_V and event X, expressed as

$$p_Y(Y_V, \mathrm{X}) = p_Y(Y_V \mid \mathrm{X})P(\mathrm{X}) = p_Y(Y_V \mid \mathrm{X}) \tag{13}$$

According to Eq. (6), three cases need to be discussed: (1) Case I: $|\Pi| \in [2f_{\max}, +\infty)$; (2) Case II: $|\Pi| \in (f_{\max}, 2f_{\max})$; (3) Case III: $|\Pi| \in (f_{\max}, +\infty)$.

(1) Case I: $|\Pi| \in [2f_{\max}, +\infty)$.

It is assumed that the probability density $p_Y(Y_V)$ caused by event Θ satisfies the normal distribution, as follows

$$Y_V \mid \Theta = Y_{V,\max} \sim N\left(\frac{2f_{\max}}{K}, \sigma\right) \tag{14}$$

The probability of event Θ is expressed as follows

$$P(\Theta) = 1 \tag{15}$$

Combining Eqs. (14) and (15), the following relationship can be obtained.

$$Y_V, \Theta = Y_V \mid \Theta \sim N\left(\frac{2f_{\max}}{K}, \sigma\right) \tag{16}$$

According to Eq. (6), the Y_V of the BLD will increase by $2x/K$ after event X occurs; thus, the $p_Y(Y_V, \mathrm{X})$ is expressed as follows

$$Y_V, \Theta, \mathrm{X} = Y_V, \Theta \mid \mathrm{X} \sim N\left(\frac{2f_{\max}}{K} + \frac{2x}{K}, \sigma\right) \tag{17}$$

Therefore, the expectation of the normal distribution can be used to identify x (i.e., the variation of $f_{\max}$) according to Eqs. (12), (16), (17), shown in Eq. (18).

$$\frac{2x}{K} = \left|E\left(Y_{V,\max}, \Theta, \mathrm{X}\right) - E\left(Y_{V,\max}, \Theta\right)\right| \tag{18}$$

(2) Case II: $|\Pi| \in (f_{\max}, 2f_{\max})$.

In this case, $P(\overline{\Theta}_3)$ is equal to 1 as follows

$$P(\overline{\Theta}_3) = 1 \tag{19}$$

Define $p_\Pi(\Pi_a, \Pi_b)$ is the joint probability density distribution of alternating VLF, and $p_Y(Y_V, \overline{\Theta}_3 | \Pi_a, \Pi_b)$ obeys the normal distribution, as follows

$$Y_V, \overline{\Theta}_3 \left| \Pi_a, \Pi_b \sim N\left(\frac{|\Pi_a| + |\Pi_b| - 2f_{\max}}{K}, \sigma^2\right)\right. \tag{20}$$

where $p_Y(Y_V, \overline{\Theta}_3, \Pi_a, \Pi_b)$ is expressed as follows

$$p_Y(Y_V, \overline{\Theta}_3, \Pi_a, \Pi_b) = p_Y(Y_V | \Pi_a, \Pi_b) \cdot p_F(\Pi_a, \Pi_b) \tag{21}$$

$p_Y(Y_V, \overline{\Theta}_3)$ is expressed as follows

$$\begin{aligned} p_Y(Y_V, \overline{\Theta}_3) &= \int p_Y(Y_V, \overline{\Theta}_3, \Pi_a, \Pi_b) \mathrm{d}\left[p_\Pi(\Pi_a, \Pi_b)\right] \\ &= \int p_Y(Y_V, \overline{\Theta}_3 \mid \Pi_a, \Pi_b) \cdot p_\Pi(\Pi_a, \Pi_b) \mathrm{d}\left[p_\Pi(\Pi_a, \Pi_b)\right] \end{aligned} \tag{22}$$

When X occurs, the probability density of $p_Y(Y_V, \overline{\Theta}_3, \Pi_a, \Pi_b | \mathrm{X})$ can be expressed as follows

$$p_Y(Y_V, \overline{\Theta}_3, \Pi_a, \Pi_b | X) = p_Y(Y_V, \overline{\Theta}_3 \left| \Pi_a, \Pi_b, X\right.) p_F(\Pi_a, \Pi_b) \tag{23}$$

According to Eq. (6), the probability density of $p_Y(Y_V, \overline{\Theta}_3 | \Pi_a, \Pi_b, \mathrm{X})$ is the result of $p_Y(Y_V, \overline{\Theta}_3 | \Pi_a, \Pi_b)$ shifted by $-2x/K$ on the Y_V coordinate axis as follows

$$Y_V, \overline{\Theta}_3 \mid \Pi_a, \Pi_b, \mathrm{X} \sim N\left(\frac{|\Pi_a| + |\Pi_b| - 2f_{\max}}{K} - \frac{2x}{K}, \sigma\right) \tag{24}$$

$p_Y(Y_V, \overline{\Theta}_3, \mathrm{X})$ is expressed as follows

$$\begin{aligned} p_Y(Y_V, \overline{\Theta}_3, \mathrm{X}) &= p_Y(Y_V, \overline{\Theta}_3 | \mathrm{X}) P(\mathrm{X}) \\ &= p_Y(Y_V, \overline{\Theta}_3 | \mathrm{X}) \\ &= \int p_Y(Y_V, \overline{\Theta}_3, \Pi_a, \Pi_b \mid \mathrm{X}) \mathrm{d}\left[p_\Pi(\Pi_a, \Pi_b)\right] \\ &= \int p_Y(Y_V, \overline{\Theta}_3 \mid \Pi_a, \Pi_b, \mathrm{X}) \cdot p_\Pi(\Pi_a, \Pi_b) \mathrm{d}\left[p_\Pi(\Pi_a, \Pi_b)\right] \end{aligned} \tag{25}$$

According to Eqs. (20), (22), (24), and (25):

$$\frac{x}{2K} = \left|E\left(Y_V, \overline{\Theta}_3, \mathrm{X}\right) - E\left(Y_V, \overline{\Theta}_3\right)\right| \tag{26}$$

The x can be represented by the absolute difference of the $E(Y_V, \overline{\Theta}_3, \mathrm{X})$ and $E(Y_V, \overline{\Theta}_3)$.

(3) Case III: $|\Pi| \in (f_{\max}, +\infty)$.

According to Eq. (11), $p_Y(Y_V)$ can be described by the one-fold normal distribution function and three other distribution functions at most, and $p_Y(Y_V | \Theta)$ is expressed as follows

$$p_Y(Y_V, \Theta) = p_Y(Y_V \mid \Theta) \cdot P(\Theta) \tag{27}$$

In Eq. (27), $P(\Theta)$ can be considered as the weight of the one–fold normal distribution. The x can be represented by the probability density weight of event Θ, which decreases as $f_{\max}$ increases, shown in Eq. (28).

$$P(\Theta) = \int_{2f_{\max}}^{+\infty} p_\Pi{}^2(|\Pi|) d\Pi > P(\Theta, \mathrm{X}) = \int_{2f_{\max}+2x}^{+\infty} p_\Pi{}^2(|\Pi|) d\Pi \tag{28}$$

In summary, the statistical characteristic of Y_V can represent the $f_{\max}$ of bearing. It is necessary to point out that the $E(Y_V)$ can describe the BWP when $p_Y(Y_V)$ fits one-dimensional normal distribution.

4. Application to BWP Assessment

4.1 Flowchart

Step1: Analyze BLD response under four vehicle driving case.
Step2: Extract the BLD variation under case B and case C.
Step3: Acquire the evaluation index.

4.2 Response of BLD under Vehicle Longitudinal Effect

The continuous steel truss railway bridge with a span arrangement of (108 + 192 + 336 + 336 + 192 + 108) m was shown in Fig. 6. Except fixed joint 4, the remaining six bearings are longitudinal spherical steel bearings. The PTFE sliding plate is the sliding part of the bearings. Each bearing was equipped with a displacement transducer, which measured the BLD with a sampling frequency of 1 Hz. Vehicle traffic sensors were installed onto the bridge deck to record vehicles driving direction. Because the bridge is a symmetrical structure, this study analyzed the half structure response on the Beijing side only.

Figure 7 Showed the response of BLD 1 – 3 (bearing 1 – 3 longitudinal displacement) at different time scales. Two pieces of

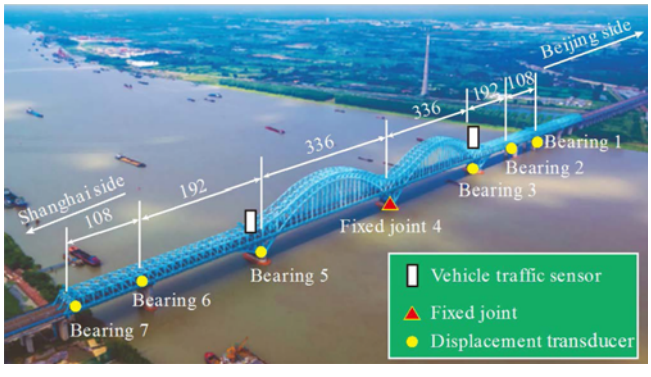

Fig. 6. The Layout of Sensors on Continuous Truss Bridge (unit: m)

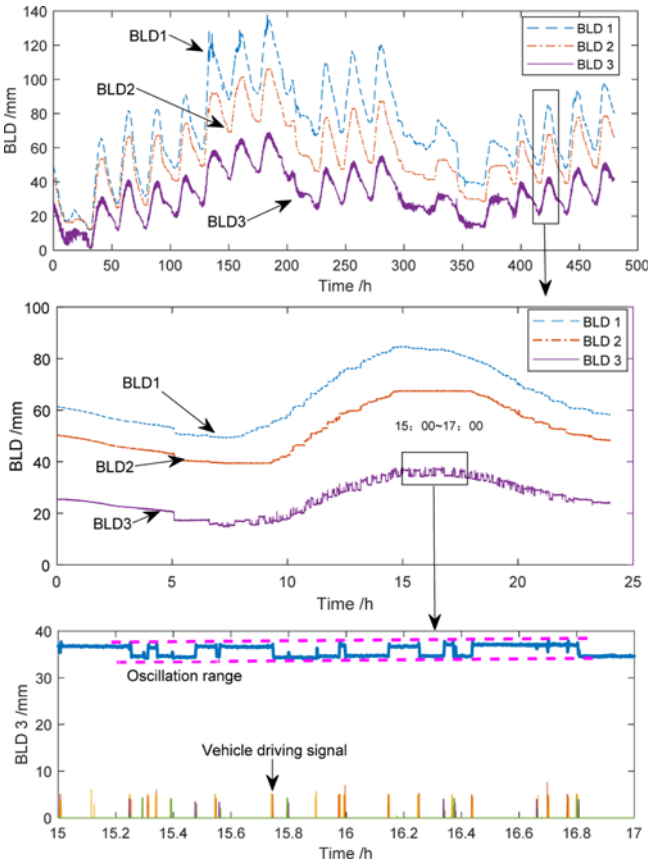

Fig. 7. Response of BLD on Different Time Scales

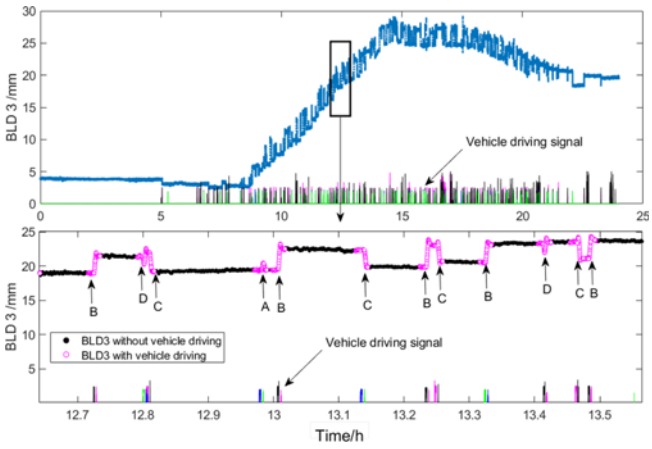

Fig. 8. Response of BLD 3 Under Different Vehicle Driving Cases

Table 2. Classification of Vehicle Driving Cases

Vehicle driving direction		Current driving direction	
		Shanghai To Beijing	Beijing To Shanghai
Previous driving direction	Shanghai to Beijing	A	B
	Beijing to Shanghai	C	D

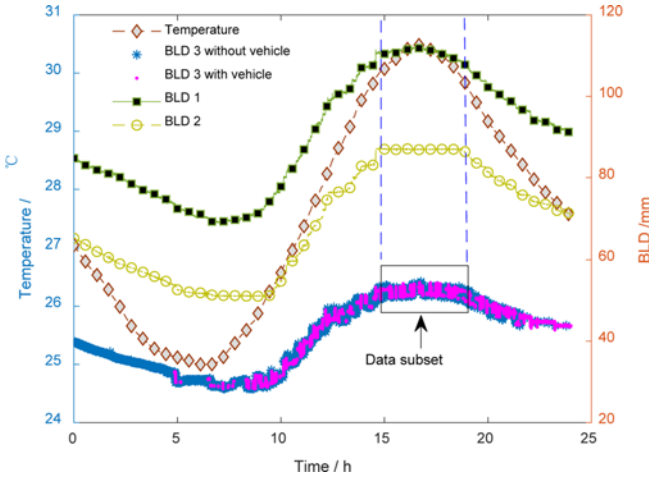

Fig. 9. Select Data Subset to Eliminate Temperature Effect

information can be obtained as follow :

1. In the 480h and 24h monitoring data, BLD 1–2 were relatively smooth, indicating BLD 1 and BLD 2 were not affected by vehicle. However, BLD 3 exhibited an obvious oscillation, which indicated that BLD 3 was affected by other factors significantly besides temperature.
2. In 15:00 – 17:00 of one day, the oscillation of BLD 3 and vehicle driving signal indicated that the BLD3 was affected by VLF significantly. Moreover, after the vehicle passed through the bridge, BLD 3 could not be restored, which implied that the bearing friction changed after the vehicle passed through bridge.

Figure 8 shows 24 h monitoring data of BLD 3. The vehicle driving cases can be recognized by the vehicle traffic sensors installed on the deck, and the classification of vehicle driving cases is presented in Table 2.

The details of BLD 3 during 12:40 – 13:40 are shown in Fig. 8 without vehicles meeting on the bridge. The oscillation of BLD 3 was induced by case B and case C, and restoration of BLD 3 was induced by case A and case B. The BLD variation was consistent with Fig. 5. Consequently, the vehicle longitudinal effect must be considered when BWP of bearing 3 is evaluated by BLD monitoring data.

4.3 Signal Extraction and Acquire Evaluation Index

The 20-day BLD monitoring data were offered (Fig. 7). To weaken the the influence of temperature on BLD, the time window with slow temperature variation everyday was selected (Fig. 9). In the period, the alternating vehicle longitudinal excitation can be regarded as an isothermal process. According to the train traffic information reconded by vehicle traffic sensors, the response of BLD 3 induced by case B and case C can be extracted in the time domain. Fig. 10 shows the probability density of the evaluation index using the normal distribution, and Fig. 11 shows quantile-quantile(Q-Q) plot for normal distribution test. $E(Y_V)$ can be obtained as follows

$$E(Y_V) = \frac{2.17 + |-2.06|}{2} = 2.12 \text{ mm} \tag{29}$$

With the degradation of the BWP, there would be an extreme

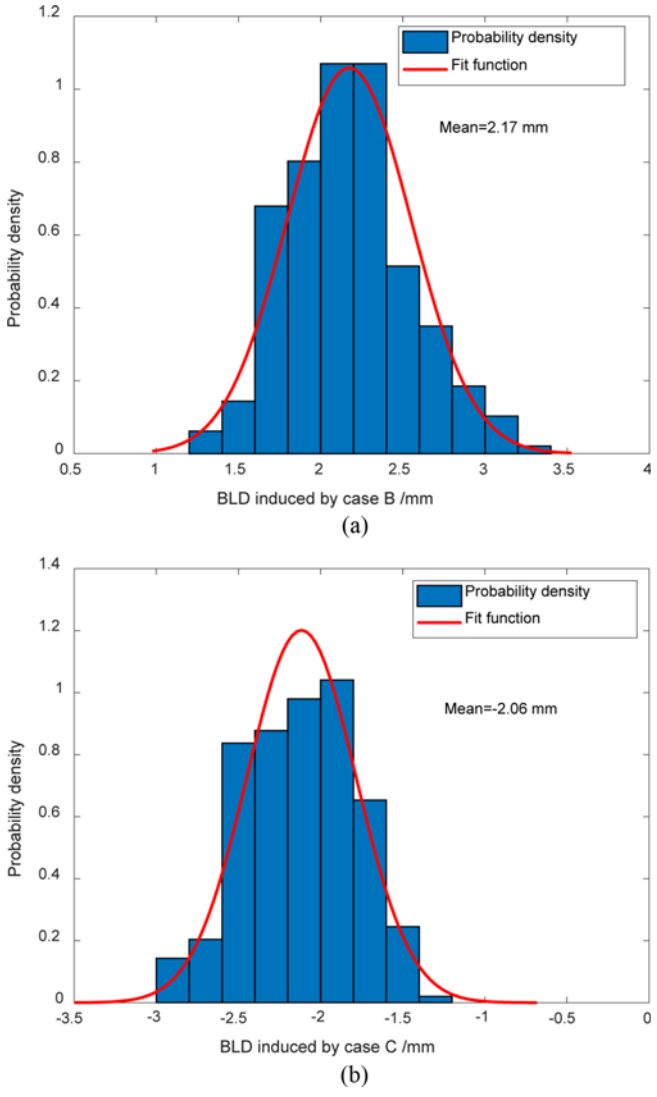

Fig. 10. Probability Density Distribution of Vehicle-Induced BLD: (a) BLD Induced by Case B, (b) BLD Induced by Case C

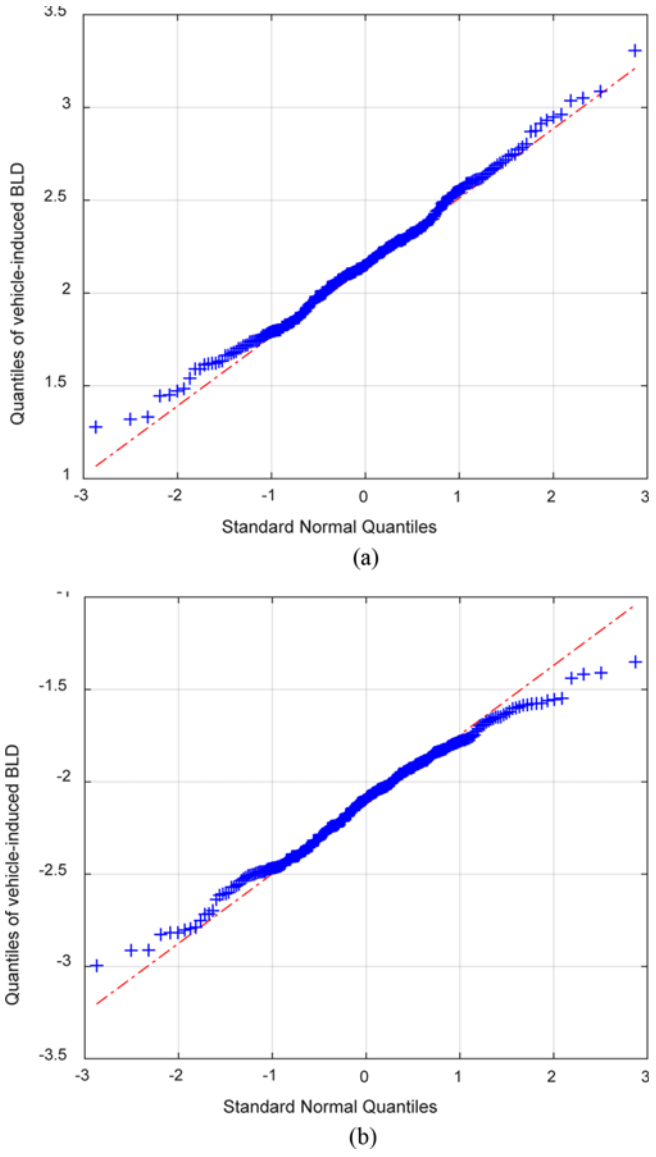

Fig. 11. Q-Q Plot of Vehicle-Induced BLD Versus Standard Normal: (a) BLD Induced by Case B Versus Standard Normall, (b) BLD Induced by Case C Versus Standard Normal

event that Y_V drops to zero, indicating that f_{max} is greater than Π, so bearing 3 should be repaired in time. The result can guide the maintenance of bearings in future.

5. Conclusions

This paper proposed a hysteresis model for VLF-induced BLD (y_F) and BLD (y), and a novel approach for BWP assessment was applied to a real-world bridge using alternating vehicle longitudinal excitation. According to the hysteresis model, the alternating VLF changes the bearing friction when $|y_{F\max}|$ is greater than f_{max}/K. In this case, f_{max} can be represented by BLD induced by alternating VLF in some ways. In addition, some suggestions were given to help the BWP assessment research in future:

1. Essentially, BWP can be evaluated by the hysteresis model composed of bearing friction and BLD. Both temperature and vehicle can affect the BLD in railway bridge; thus, on one hand, BWP assessment using TDRM is credible only if the vehicle effect is negligible. On the other hand, the BWP assessment using alternating vehicle longitudinal excitation is feasible when temperature effect can be suppressed.
2. Highway bridges are more flexible than railway bridges, and vehicles load has significant effects on longitudinal displacement. The high-frequency excitation of vehicle may change the expansion joint friction frequently. Therefore, the dependability of TDRM for expansion joint assessment needs to be confirmed in highway bridges when longitudinal displacement induced by vehicle is significant.

Acknowledgments

This study was jointly supported from the National Key Research and Development Project of China under Grant Nos.

2016YFB1200401-107; The Key Research and Development Project of Hebei Province (CN) under Grant Nos. 19210804D; Innovative Research Group Project of the Natural Science Foundation of Hebei Province (CN) under Grant Nos. E2021210099; The Natural Science Foundation of Hebei Province (CN) under Grant Nos. E2020210022; The Natural Science Foundation for Youths of Hebei Province (CN) under Grant Nos.E2021210055.

ORCID

Not Applicable

References

Alexander J, Yarnold M (2020) Quasi-static bearing evaluation and monitoring — A case study. *Frontiers in Built Environment* 6:69, DOI: 10.3389/fbuil.2020.00069

Brownjohn JMW, Koo K-Y, Scullion A, List D (2015) Operational deformations in long-span bridges. *Structure and Infrastructure Engineering* 11:556-574, DOI: 10.1080/15732479.2014.951857

Chen Z-H, Liu X-W, Zhou G-D, Liu H, Fu Y-X (2021) Damage detection for expansion joints of a combined highway and railway bridge based on long-term monitoring data. *Journal of Performance of Constructed Facilities* 35(4):04021037, DOI: 10.1061/(ASCE)CF.1943-5509.0001608

Filipov ET, Fahnestock LA, Steelman JS, Hajjar JF, LaFave JM, Foutch DA (2013) Evaluation of quasi-isolated seismic bridge behavior using nonlinear bearing models. *Engineering Structures* 49:168-181, DOI: 10.1016/J.ENGSTRUCT.2012.10.011

Garcia-Sanchez D, Fernandez-Navamuel A, Sánchez DZ, Alvear D, Pardo D (2020) Bearing assessment tool for longitudinal bridge performance. *Journal of Civil Structural Health Monitoring* 10(5):1023-1036, DOI: 10.1007/s13349-020-00432-1

Guo T, Liu J, Huang L (2016) Investigation and control of excessive cumulative girder movements of long-span steel suspension bridges. *Engineering Structures* 125:217-226, DOI: 10.1016/J.ENGSTRUCT.2016.07.003

Han Q, Qian M, Xu J, Liu M (2021a) Structural health monitoring research under varying temperature condition: A review. *Journal of Civil Structural Health Monitoring* 11:1-25, DOI: 10.1007/s13349-020-00444-x

Han N, Zhao W, Zhang B, Zhang H, Zhou L (2021b) Performance assessment of railway multispan steel truss bridge bearing by thermal excitation. *Journal of Civil Structural Health Monitoring* 12(1):163-178, DOI: 10.1007/s13349-021-00532-6

Huang H-B, Yi T-H, Li H-N, Liu H (2018) New representative temperature for performance alarming of bridge expansion joints through temperature-displacement relationship. *Journal of Bridge Engineering* 23(7):04018043.1-04018043.14, DOI: 10.1061/(ASCE)BE.1943-5592.0001258

Jia Y, Zhao R, Liao P, Li F (2018) Influence of friction effect of sliding bearings on seismic response of continuous beam bridge. *Journal of Tongji University (Natural Science)* 46(5):580-587, DOI: 10.11908/j.issn.0253-374x.2018.05.003

Li X, Xiao Y, Guo H, Zhang J (2022) A BIM based approach for structural health monitoring of bridges. *KSCE Journal of Civil Engineering* 26(1):155-165, DOI: 10.1007/s12205-021-2040-3

Liang Y, Feng Q, Fu M, Wu B, Lu J, Tang G (2022) Prediction and monitoring of the construction vibration effect on an adjacent old long span double-convex arch bridge. *KSCE Journal of Civil Engineering* 26(5):2183-2201, DOI: 10.1007/s12205-022-2170-2

Lima J, Brito J (2009) Inspection survey of 150 expansion joints in road bridges. *Engineering Structures* 31:1077-1084, DOI: 10.1016/j.engstruct.2009.01.011

Liu W, Dai G, Qin H (2019) Influence of friction effect of sliding bearing on track-bridge interaction between continuous welded rail and long-span bridge in high-speed railway. *Journal of Central South University* 50(3):627-633, DOI: 10.11817/j.issn.1672-7207.2019.03.016

Murphy B, Yarnold M (2018) Temperature-driven structural identification of a steel girder bridge with an integral abutment. *Engineering Structures* 155:209-221, DOI: 10.1016/J.ENGSTRUCT.2017.10.074

Ni Y, Hua X, Wong K, Ko J (2007) Assessment of bridge expansion joints using long-term displacement and temperature measurement. *Journal of Performance of Constructed Facilities - J Perform Constr Facil* 21:143-151, DOI: 10.1061/(ASCE)0887-3828(2007)21:2(143)

Ni YQ, Wang Y-W, Zhang C (2020) A Bayesian approach for condition assessment and damage alarm of bridge expansion joints using long-term structural health monitoring data. *Engineering Structures* 212:110520, DOI: 10.1016/j.engstruct.2020.110520

Quaglini V, Gandelli E, Dubini P (2018) Influence of the static friction on the seismic response of a building isolated with sliding bearings. 16th European Conference on Earthquake Engineering (16ECEE)

Srinivas V, Ramanjaneyulu K, Kumar KS, Parivallal S, Kesavan K, Ravisankar KL, Lakshmanan N, Iyer NR (2013) Evaluation of longitudinal force on a railway bridge based on strain measurements. *Experimental Techniques* 37:55-67, DOI: 10.1111/j.1747-1567.2011.00747.x

Sun Z, Zhang Y (2016) Failure mechanism of expansion joints in a suspension bridge. *Journal of Bridge Engineering* 21:05016005, DOI: 10.1061/(ASCE)BE.1943-5592.0000942

Wang G-X, Ding Y-L, Song Y-S, Wu L-Y, Yue Q, Mao G-H (2015) Detection and location of the degraded bearings based on monitoring the longitudinal expansion performance of the main girder of the dashengguan yangtze bridge. *Journal of Performance of Constructed Facilities* 30:04015074, DOI: 10.1061/(ASCE)CF.1943-5509.0000820

Wen J, Han Q, Du X (2019) Shaking table tests of bridge model with friction sliding bearings under bi-directional earthquake excitations. *Structure and Infrastructure Engineering* 15:1264-1278, DOI: 10.1080/15732479.2019.1618350

Wu G-M, Yi T, Yang D-H, Li H, Liu H (2021) Early warning method for bearing displacement of long-span bridges using a proposed time-varying temperatur – displacement model. *Journal of Bridge Engineering* 26:04021068, DOI: 10.1061/(ASCE)BE.1943-5592.0001763

Xia Q, Xia Y, Wan H-P, Zhang J, Ren W-X (2020) Condition analysis of expansion joints of a long-span suspension bridge through metamodel-based model updating considering thermal effect. *Structural Control and Health Monitoring* 27, DOI: 10.1002/stc.2521

Yarnold M, Moon F (2015) Temperature-based structural health monitoring baseline for long-span bridges. *Engineering Structures* 86, DOI: 10.1016/j.engstruct.2014.12.042

Yarnold MT, Moon FL, Aktan AE (2015) Temperature-based structural identification of long-span bridges. *Journal of Structural Engineering* 141(11):04015027.1-04015027.10, DOI: 10.1061/(ASCE)ST.1943-541X.0001270

Yue L, Kehai W, Qiqi W (2017) Experiment of ultimate shear failure and friction sliding performance of rubber bearings of bridges. *The Open Civil Engineering Journal* 11:586-597, DOI: 10.2174/1874149501711010586